

# Light-cone velocities after a global quench in a non-interacting model

K. Najafi,<sup>1</sup> M. A. Rajabpour,<sup>2</sup> and J. Viti<sup>3</sup>

<sup>1</sup>*Department of Physics, Georgetown University, 37th and O Sts. NW, Washington, DC 20057, USA*

<sup>2</sup>*Instituto de Física, Universidade Federal Fluminense,  
Av. Gal. Milton Tavares de Souza s/n, Gragoatá, 24210-346, Niterói, RJ, Brazil*

<sup>3</sup>*ECT & Instituto Internacional de Física, UFRN,  
Campos Universitário, Lagoa Nova 59078-970 Natal, Brazil*

(Dated: February 28, 2024)

We study the light-cone velocity for global quenches in the non-interacting XY chain starting from a class of initial states that are eigenstates of the local  $z$ -component of the spin. We point out how translation invariance of the initial state can affect the maximal speed at which correlations spread. As a consequence the light-cone velocity can be state-dependent also for non-interacting systems: a new effect of which we provide clear numerical evidence and analytic predictions. Analogous considerations, based on numerical results, are drawn for the evolution of the entanglement entropy.

## I. INTRODUCTION

In a seminal contribution Lieb and Robinson<sup>1</sup> proved that in a non-relativistic quantum spin system, the operator norm of the commutator between two local observables  $\hat{A}(\mathbf{x}, t)$  and  $\hat{B}(\mathbf{y}, 0)$  is exponentially small as long as  $|\mathbf{x} - \mathbf{y}| \geq v_{LR}t$ , for some  $v_{LR} > 0$ <sup>2-4</sup>. The bound reads

$$||[\hat{A}(\mathbf{x}, t), \hat{B}(\mathbf{y}, 0)]|| \leq c ||\hat{A}|| ||\hat{B}|| e^{-(|\mathbf{x} - \mathbf{y}| - v_{LR}t)/\xi}, \quad (1)$$

where  $||\hat{O}||$  is the aforementioned operator norm of the observable  $\hat{O}$ ;  $c$  and  $\xi$  are constants. The Lieb-Robinson theorem holds in any dimension and for a translation invariant Hamiltonian with interactions decaying sufficiently fast (exponentially or superexponentially) with the distance. The parameter  $v_{LR}$  is called Lieb-Robinson velocity and depends only on the Hamiltonian<sup>1-4</sup> driving the time evolution; in particular it is state-independent<sup>5</sup>. The existence of a finite  $v_{LR}$  implies that information cannot propagate arbitrary fast<sup>1</sup>. The Lieb-Robinson result represents nowadays a powerful tool to prove rigorous bounds for correlation and entanglement growth<sup>6</sup>. It is relevant for estimating the computational complexity, or simulability, of a system<sup>6,7</sup> and provides a link between the presence of a gap and short length correlations<sup>4,8,9</sup>.

Moreover, formidable experimental<sup>10-14</sup> and theoretical (for an overview<sup>15-18</sup>) progress in many-body quantum dynamics, have further underlined its striking physical implications. Among them, the emergence of light-cone effects in correlation functions of time-evolved local observables for systems that are not manifestly Lorentz invariant, like quantum spin chains<sup>19-23,25-29</sup>. For instance, the Lieb-Robinson theorem has been invoked to explain the ballistic spreading of correlation functions in paradigmatic condensed matter models such as the XXZ spin chain<sup>30</sup> or the Hubbard model<sup>31</sup> after a global quench; see also<sup>32</sup> for a pedagogical survey. Similar considerations apply to the linear growth of the entanglement entropies<sup>33-41</sup>. Quantitative predictions on the spreading of correlations and the entanglement entropy are also of clear experimental interest; see<sup>42-45</sup> for experimental verifications of light-cone effects in many-body

systems. A complementary physical interpretation of these emergent phenomena is based on the idea<sup>46,47</sup> that in a quench problem the initial state acts as a source of pairs of entangled quasi-particles. The quasi-particles have opposite momenta and move ballistically; see<sup>48-50</sup> for applications to integrable models. Recently it has also been pointed out that light-cone effects can be recovered from field theoretical arguments without relying on particular properties of the post-quench quasi-particle dynamics<sup>51</sup>.

It is important to stress that the Lieb-Robinson theorem proves the existence of a maximal velocity for correlations to develop. However the observed propagation velocity is actually state-dependent and non-trivially predictable. In other words, it is not directly related to  $v_{LR}$  that rather furnishes an upper bound. For one-dimensional spin chains, a state-dependent light-cone velocity was noticed first in<sup>30</sup>. In a context of integrability, it was pointed out how the dispersions of the quasi-particles in the stationary state<sup>52</sup> (the so-called Generalized Gibbs Ensemble<sup>53,54</sup>) was initial state dependent. A prediction for their velocities was then proposed and numerically tested. This idea has lead to many subsequent crucial developments in the field<sup>48,49,55-57</sup>. In the simpler setting of a non-interacting model, where quasi-particles are characterized by a dispersion relation  $\varepsilon_k$  there is a maximum group velocity  $v_g$  allowed by the dispersion. To our best knowledge, in all the examples considered in the literature so far (for example<sup>21-23,59,60</sup>) correlations were found to spread with a light-cone velocity given by  $v_g$  independently of the initial state. In this paper we point out for the first time that even if the dispersion of the quasi-particles after the quench is not affected by the initial state, its symmetries and in particular translation invariance can introduce additional selection rules on the momenta of the quasi-particles. As a consequence the light-cone velocity can be state-dependent and smaller than  $v_g$  also in a non-interacting model

The paper is organized as follows. In Sec. II and Sec. III we introduce the XY spin chain and discuss a special class of initial states for which time-evolution of local observables can be calculated easily. In Sec. IV and VI we

analyze the propagation velocity both for physical two-point correlation functions and the entanglement entropy. In Sec. V we show how fermionic correlation functions at the edge of the light-cone can be approximated by combinations of Airy functions. Similar statements were also made in<sup>24,25</sup> for related many-body quench problems. After the conclusions in Sec. VII, one appendix completes the paper.

## II. XY CHAIN: NOTATIONS AND INITIAL STATES

In this section, we briefly remind the XY chain, its fermionic representation and we then introduce the initial states discussed in the rest of the paper. The Hamiltonian of the XY-chain<sup>58</sup> is

$$\begin{aligned} \mathbf{H}_{XY} = & -J \sum_{l=1}^L \left[ \left( \frac{1+\gamma}{2} \right) \sigma_l^x \sigma_{l+1}^x + \left( \frac{1-\gamma}{2} \right) \sigma_l^y \sigma_{l+1}^y \right] \\ & - Jh \sum_{l=1}^L \sigma_l^z, \end{aligned} \quad (2)$$

where the  $\sigma_l^\alpha$  ( $\alpha = x, y, z$ ) are Pauli matrices and  $J, \gamma, h$  are real parameters; in particular  $J > 0$  and conventionally  $h$  is called magnetic field. The XY model reduces to the Ising spin chain for  $\gamma = 1$  and it is the XX chain when  $\gamma = 0$ . We will also choose periodic boundary conditions for the spins, i.e.  $\sigma_l^\alpha = \sigma_{l+L}^\alpha$ . Introducing canonical spinless fermions through the Jordan-Wigner transformation,  $c_l^\dagger = \prod_{n<l} \sigma_n^z \sigma_l^+$ , (2) becomes

$$\mathbf{H}_{XY} = J \sum_{l=1}^L (c_l^\dagger c_{l+1} + \gamma c_l^\dagger c_{l+1}^\dagger + h.c.) - Jh \sum_{l=1}^L (2c_l^\dagger c_l - 1) \quad (3)$$

where  $c_{L+1}^\dagger = -\mathcal{N} c_1^\dagger$ . Here  $\mathcal{N} = \pm 1$  is the eigenvalue of operator  $\prod_{l=1}^L \sigma_l^z$  that is conserved fermion parity. The above Hamiltonian can be written as

$$\mathbf{H}_{XY} = \mathbf{c}^\dagger \mathbf{A} \mathbf{c} + \frac{1}{2} \mathbf{c}^\dagger \mathbf{B} \mathbf{c}^\dagger + \frac{1}{2} \mathbf{c} \mathbf{B}^T \mathbf{c} - \frac{1}{2} \text{Tr} \mathbf{A}, \quad (4)$$

with appropriate real matrices  $\mathbf{A}$  and  $\mathbf{B}$  that are symmetric and antisymmetric, respectively. In the sector with an even number of fermions ( $\mathcal{N} = 1$ ), the so-called Neveu-Schwartz sector, the Hamiltonian can be diagonalized in Fourier space by a unitary Bogoliubov transformation. In particular, there are no subtleties related to the appearance of a zero-mode. Writing (3) in the Fourier space and then Bogoliubov transformation leads to

$$\mathbf{H}_{XY} = \sum_{k=1}^L \varepsilon_k (b_k^\dagger b_k - \frac{1}{2}). \quad (5)$$

The canonical Bogoliubov fermions  $b$ 's have the following dispersion relation and group velocities

$$\varepsilon_k = 2J \sqrt{(\cos \phi_k - h)^2 + \gamma^2 \sin^2 \phi_k}, \quad (6)$$

$$v_k = 2J \sin \phi_k \frac{\gamma^2 \cos \phi_k - \cos \phi_k + h}{\sqrt{(\cos \phi_k - h)^2 + \gamma^2 \sin^2 \phi_k}}, \quad (7)$$

where  $\phi_k = \frac{2\pi}{L}(k - \frac{1}{2})$  and  $k = 1, \dots, L$ . We will assume  $L$  even from now on. The diagonalization procedure will be also briefly revisited in Sec. III.

In this paper, we are interested to study the time evolution of such a system from initial states that are eigenstates of the local  $\sigma_j^z$  operators. For example, the initial state  $|\psi_0\rangle$  can be a state with all spins pointing up (no fermions) or down (one fermion per lattice site); other possibilities can be the Néel state  $|\downarrow\uparrow\downarrow\uparrow \dots \downarrow\uparrow\rangle$  and alike. Moreover, all the states that we study have a periodic pattern in real space with a fixed number of spin up. We label our crystalline initial states  $|\psi_0\rangle$  as  $(r, s)$ , where  $r$  is the spin up (fermion) density and  $s$  is the number of spin up in the unit cell of the crystal. For example, the Néel state is labeled by  $(\frac{1}{2}, 1)$  and the state  $|\downarrow\downarrow\uparrow\uparrow\downarrow\downarrow \dots \downarrow\downarrow\uparrow\uparrow\rangle$  will be  $(\frac{1}{2}, 2)$ . It is also convenient to define  $p \equiv \frac{s}{r}$  that for simplicity we restrict to be a positive integer (i.e.  $s$  is a multiple of  $r$ ). Although the class of initial state considered is not comprehensive, it turns out to be enough for the upcoming discussion.

## III. EVOLUTION OF THE CORRELATION FUNCTIONS

Light-cone effects can be studied, monitoring the connected correlation function of the  $z$ -component of the spin  $S^z = \sigma^z/2$ ,

$$\Delta_{ln}(t) = \langle S_l^z(t) S_n^z(t) \rangle - \langle S_l^z(t) \rangle \langle S_n^z(t) \rangle. \quad (8)$$

For our initial states, (8) is zero at time  $t = 0$ ; however, according to<sup>1</sup>, after a certain time which depends on  $|l - n|$ , it starts to change significantly.

For instance<sup>30</sup>, such a time can be chosen as the first inflection point  $\tau$ . Varying  $|l - n|$  in Eq. (8), one can numerically evaluate  $\tau$  and provide a prediction for the speed  $v_{\max}$  at which information spreads in the system determining the ratio  $\frac{|l-n|}{2\tau}$ . We will call  $v_{\max}$  the light-cone velocity. According to a quasi-particle picture of the quench dynamics<sup>21-23,46-49,59,60</sup>, for a translation invariant Hamiltonian the initial state  $|\psi_0\rangle$  acts as a source of pairs of entangled quasi-particles with opposite momenta. In absence of interactions, the quasi-particles move ballistically with a group velocity fixed by their dispersion relation. Within this framework,  $\tau$  is state-independent and  $v_{\max} = v_g$  where  $v_g > 0$  is the maximum over the  $k$ 's of Eq. (7). We will actually show that  $v_g$  is rather an upper bound for the observed  $v_{\max}$ , which can indeed be dependent on the symmetries of the initial

Generic Quadratic Hamiltonian
$\mathbf{T}_{11}, \mathbf{T}_{12}, \mathbf{T}_{21}$ and $\mathbf{T}_{22}$ are complex matrices.
$\mathbf{T}_{21} = (\mathbf{T}_{12})^*$
$\mathbf{T}_{22} = (\mathbf{T}_{11})^*$
$(\mathbf{T}_{11})^T = \mathbf{T}_{11}$
$(\mathbf{T}_{22})^T = \mathbf{T}_{22}$
$\mathbf{T}_{22}\mathbf{T}_{12} + \mathbf{T}_{21}\mathbf{T}_{22} = 0$

TABLE I. Properties of the four  $L \times L$  blocks of the matrix  $\mathbf{T}$  for a quadratic Hamiltonian (4). The notation is obvious and time dependence is omitted here.

state. Finally note that in absence of interactions, the light-cone velocity is independent on finite size effects as long as  $L \gg |l - n|$ .

To study the time-evolution of the correlation function (8), first, we need to analyze the propagators

$$F_{ln}(t) = \langle \psi_0 | c_l^\dagger(t) c_n^\dagger(t) | \psi_0 \rangle, \quad (9)$$

$$C_{ln}(t) = \langle \psi_0 | c_l(t) c_n^\dagger(t) | \psi_0 \rangle, \quad (10)$$

where  $|\psi_0\rangle$  is a state of the type introduced in Sec. II. If there is no ambiguity, we will drop it from the expectation values. From Eqs. (9)-(10) and the Wick theorem, which applies to our states<sup>61</sup>, it follows

$$\Delta_{ln}(t) = |F_{ln}(t)|^2 - |C_{ln}(t)|^2. \quad (11)$$

Note that as  $L \times L$  matrices whose matrix elements are given in Eqs. (9)-(10),  $\mathbf{F}$  and  $\mathbf{C}$  satisfy  $\mathbf{F}^T = -\mathbf{F}$  and  $\mathbf{C}^\dagger = \mathbf{C}$ .

It is straightforward to show that for a fermionic model with a quadratic Hamiltonian as in Eq. (4) one has,

$$\begin{pmatrix} \mathbf{c}(t) \\ \mathbf{c}^\dagger(t) \end{pmatrix} = \underbrace{e^{-it \begin{pmatrix} \mathbf{A} & \mathbf{B} \\ -\mathbf{B} & -\mathbf{A} \end{pmatrix}}}_{\mathbf{T}(t)} \begin{pmatrix} \mathbf{c}(0) \\ \mathbf{c}^\dagger(0) \end{pmatrix} \quad (12)$$

where  $\mathbf{c} = \{c_1, c_2, \dots, c_L\}$  and  $\mathbf{c}^\dagger = \{c_1^\dagger, c_2^\dagger, \dots, c_L^\dagger\}$  are vectors of length  $L$ ; i.e.  $\mathbf{T}$  is a  $2L \times 2L$  matrix. Exploiting the properties of the four  $L \times L$  blocks of the matrix  $\mathbf{T}$  collected in Tab. III, Eq. (12) can be written as,

$$\begin{pmatrix} \mathbf{c}(t) \\ \mathbf{c}^\dagger(t) \end{pmatrix} = \begin{pmatrix} \mathbf{T}_{22}^*(t) & \mathbf{T}_{12}(t) \\ \mathbf{T}_{12}^*(t) & \mathbf{T}_{22}(t) \end{pmatrix} \begin{pmatrix} \mathbf{c}(0) \\ \mathbf{c}^\dagger(0) \end{pmatrix}. \quad (13)$$

Finally, after some easy algebra, explicit expression for the time-evolved matrices  $\mathbf{F}$  and  $\mathbf{C}$  can be computed and read respectively (time dependence is dropped from the  $\mathbf{T}$ 's)

$$\begin{aligned} \mathbf{F}(t) = & \mathbf{T}_{12}^* \mathbf{F}^\dagger(0) \mathbf{T}_{12}^\dagger + \mathbf{T}_{12}^* \mathbf{C}(0) \mathbf{T}_{22} + \mathbf{T}_{22} \mathbf{T}_{12}^\dagger \\ & - \mathbf{T}_{22} \mathbf{C}^T(0) \mathbf{T}_{12}^\dagger + \mathbf{T}_{22} \mathbf{F}(0) \mathbf{T}_{22}, \end{aligned} \quad (14)$$

$$\begin{aligned} \mathbf{C}(t) = & \mathbf{T}_{22}^* \mathbf{F}^\dagger(0) \mathbf{T}_{12}^\dagger + \mathbf{T}_{22}^* \mathbf{C}(0) \mathbf{T}_{22} + \mathbf{T}_{12} \mathbf{T}_{12}^\dagger \\ & - \mathbf{T}_{12} \mathbf{C}^T(0) \mathbf{T}_{12}^\dagger + \mathbf{T}_{12} \mathbf{F}(0) \mathbf{T}_{22}. \end{aligned} \quad (15)$$

Eqs. (14)-(15) are valid in principle for any free fermionic systems with Hamiltonian (4); however, they have much simpler forms in the XY chain for our particular choice of initial states as we now discuss.

In the periodic XY chain, it turns out  $[\mathbf{A}, \mathbf{B}] = 0$ ; these matrices are indeed trivially diagonalized by the unitary transformation with elements  $U_{lk} = \frac{1}{\sqrt{L}} e^{-il\phi_k}$  and  $\phi_k$  given, for  $\mathcal{N} = 1$ , below Eq. (7). Consequently, the four blocks of  $\mathbf{T}$  are mutually commuting and this leads to further simplifications. In particular, it is easy to verify that

$$\mathbf{T}_{11} = \cos[t\sqrt{\mathbf{A}^2 - \mathbf{B}^2}] - \frac{i\mathbf{A}}{\sqrt{\mathbf{A}^2 - \mathbf{B}^2}} \sin[t\sqrt{\mathbf{A}^2 - \mathbf{B}^2}], \quad (16)$$

$$\mathbf{T}_{12} = \frac{-i\mathbf{B}}{\sqrt{\mathbf{A}^2 - \mathbf{B}^2}} \sin[t\sqrt{\mathbf{A}^2 - \mathbf{B}^2}]. \quad (17)$$

The other two blocks can be found observing that  $\mathbf{T}_{22} = \mathbf{T}_{11}^*$  and  $\mathbf{T}_{21} = -\mathbf{T}_{12}$ . The eigenvalues of the matrices  $\mathbf{A}$  and  $\mathbf{B}$  are

$$\lambda_k^A = 2J(-h + \cos \phi_k), \quad (18)$$

$$\lambda_k^B = -2iJ\gamma \sin \phi_k. \quad (19)$$

From Eqs. (18)-(19) and comparing with Eq. (6), it follows  $\varepsilon_k = \sqrt{(\lambda_k^A)^2 - (\lambda_k^B)^2}$ . Recalling then Eqs.(16)-(17) we finally obtain

$$\lambda_k^{T_{11}} = [\lambda_k^{T_{22}}]^* = \cos(t\varepsilon_k) - i \frac{\lambda_k^A}{\varepsilon_k} \sin(t\varepsilon_k) \quad (20)$$

$$\lambda_k^{T_{12}} = -\lambda_k^{T_{21}} = -i \frac{\lambda_k^B}{\varepsilon_k} \sin(t\varepsilon_k). \quad (21)$$

The time-evolved matrices  $\mathbf{F}(t)$  and  $\mathbf{C}(t)$  can now be calculated for the class of representative initial states  $|\psi_0\rangle$  introduced in Sec. II. A trivial case is  $|\psi_0\rangle = |\downarrow\downarrow \dots \downarrow\downarrow\rangle$ , i.e. a state without fermions; here  $\mathbf{F}(0) = \mathbf{0}$  and  $\mathbf{C}(0) = \mathbf{1}$ . Then using unitarity of the matrix  $\mathbf{T}$  we obtain

$$[\mathbf{F}(t)]_{ln} = \frac{1}{L} \sum_{k=1}^L \lambda_k^{T_{22}} \lambda_k^{T_{12}} e^{-i\phi_k(l-n)} \quad (22)$$

$$[\mathbf{C}(t)]_{ln} = \delta_{ln} - \frac{1}{L} \sum_{k=1}^L (\lambda_k^{T_{12}})^2 e^{-i\phi_k(l-n)}. \quad (23)$$

According to Eqs. (20)-(23), the time evolution of  $\Delta_{ln}(t)$  in Eq. (8) is described by the ballistic spreading of quasi-particles with dispersion relation  $\varepsilon_k$  as in (6). As it can be also easily checked numerically, correlations spread at the maximum group velocity  $v_g$  obtained from (7), in agreement with a standard quasi-particle interpretation.

For the initial states labeled by  $(1/p, 1)$ , the matrix  $\mathbf{C}(0)$  has elements

$$[\mathbf{C}(0)]_{ln} = \delta_{ln} \left[ 1 - \frac{1}{p} \sum_{j=0}^{p-1} e^{-2\pi i \frac{lj}{p}} \right], \quad (24)$$

whereas  $\mathbf{F}(0) = \mathbf{0}$ . From the expressions in Eqs. (14)-(15) and inserting the unitary matrix  $U$  that diagonalize simultaneously all four blocks of  $\mathbf{T}$  we derive

$$\begin{aligned} [\mathbf{F}(t)]_{ln} &= \frac{1}{L} \sum_{k=1}^L \lambda_k^{T_{12}^*} \lambda_k^{T_{22}} e^{-i\phi_k(l-n)} \\ &\quad - \frac{1}{Lp} \sum_{j=0}^{p-1} e^{-\frac{2\pi i n j}{p}} \sum_{k=1}^L \lambda_k^{T_{12}^*} \lambda_{-\frac{Lj}{p}+k}^{T_{22}} e^{-i\phi_k(l-n)} \\ &\quad + \frac{1}{Lp} \sum_{j=0}^{p-1} e^{-\frac{2\pi i n j}{p}} \sum_{k=1}^L \lambda_k^{T_{22}} \lambda_{-\frac{Lj}{p}+k}^{T_{12}} e^{-i\phi_k(l-n)}, \quad (25) \end{aligned}$$

and

$$\begin{aligned} [\mathbf{C}(t)]_{ln} &= \frac{1}{L} \sum_{k=1}^L |\lambda_k^{T_{22}}|^2 e^{-i\phi_k(l-n)} \\ &\quad - \frac{1}{Lp} \sum_{j=0}^{p-1} e^{-\frac{2\pi i n j}{p}} \sum_{k=1}^L \lambda_k^{T_{22}^*} \lambda_{-\frac{Lj}{p}+k}^{T_{22}} e^{-i\phi_k(l-n)} \\ &\quad + \frac{1}{Lp} \sum_{j=0}^{p-1} e^{-\frac{2\pi i n j}{p}} \sum_{k=1}^L \lambda_k^{T_{12}} \lambda_{-\frac{Lj}{p}+k}^{T_{12}^*} e^{-i\phi_k(l-n)}. \quad (26) \end{aligned}$$

It should be noticed that for  $p = 2$  the terms in the first lines of Eqs. (25)-(26) are canceled by the  $j = 0$  contribution in the sum. The latter observation follows from

$$\lambda_k^{T_{22}^*} \lambda_{-k}^{T_{22}} + (\lambda_k^{T_{12}})^2 = 1, \quad (27)$$

that is a consequence of the unitarity of the matrix  $\mathbf{T}$  and it will be useful in our analysis of the light-cone velocities. In the next section, we will pass to study Eqs. (25)-(26) in details.

A similar study of the Eq. (8) can be also carried out for the initial states labeled by  $(s/p, s)$  where  $\mathbf{C}(0)$  has matrix elements

$$[\mathbf{C}(0)]_{ln} = \delta_{ln} \left[ 1 - \frac{1}{p} \sum_{j=0}^{p-1} \sum_{l'=0}^{s-1} e^{-2\pi i \frac{(l+l')j}{p}} \right]; \quad (28)$$

we will also briefly investigate such a possibility.

#### IV. LIGHT-CONE VELOCITIES FOR THE SIGNAL $\Delta_{ln}(t)$

In this section we extract the light-cone velocity  $v_{\max}$  for the connected two-point correlation function (8) in the XY chain. We divide our presentation in three subsections. We first focus on XX chain ( $\gamma = h = 0$ ), where an exhaustive classification can be performed and then study quenches from the Néel state ( $p = 2$ ) where also a complete picture emerges. Finally in the last subsection we examine quenches from states with  $p > 2$  where the calculation of the light-cone velocities is considerably more involved and show an example for the Ising chain.

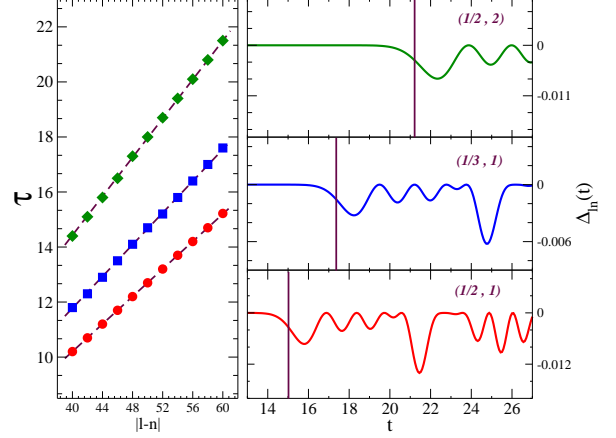


FIG. 1. (color online) On the right panel  $\Delta_{ln}(t)$  for the XX chain ( $\gamma = h = 0$ ) and  $J = -1$  with different initial states; here we have  $L = 144$  and  $|l - n| = 60$ . Vertical bars in correspondence of  $\frac{|l-n|}{2v_{\max}}$ . On the left panel we plotted the numerically estimated inflection points  $\tau$  of the signals as a function of the distances  $|l - n|$ . The points align on a straight line with slope given in Eq. (32).

##### A. Free fermions ( $J = -1, \gamma = 0$ )

We consider preliminary the simple case of the XX chain ( $\gamma = h = 0$  and  $J = -1$ ) where the fermion number is conserved and  $\mathbf{B}$  (and  $\mathbf{F}$ ) vanishes. Then the matrix  $\mathbf{C}$  for the initial states labeled by  $(1/p, 1)$  can be rewritten as

$$C_{ln} = \delta_{ln} - \frac{1}{Lp} \sum_{j=0}^{p-1} e^{-\frac{2\pi i n j}{p}} \sum_{k=1}^L e^{-i \left[ \phi_k(l-n) + \left( \varepsilon_k - \varepsilon_{\frac{Lj}{p}-k} \right) t \right]}, \quad (29)$$

where  $\varepsilon_k = -2 \cos \phi_k$  and  $\phi_k = \frac{2\pi k}{L}$  ( $k = 1, \dots, L$ ). Notice also that  $v_g = 2$ . For the sake of determining the light-cone velocity, the last exponential in Eq. (29) implies that

$$\varepsilon_{k,j}^{\text{eff}}(p) \equiv \frac{1}{2} \left( \varepsilon_k - \varepsilon_{\frac{Lj}{p}-k} \right), \quad (30)$$

can be interpreted as an effective dispersion relation for the signal. The effective dispersion originates from the discrete translational symmetry of  $p$  lattice sites of the initial state that allows multiplets of quasi-particles to be produced with momenta  $k$  and  $\frac{Lj}{p} - k$ ,  $j = 1, \dots, p$  (i.e. relaxing the condition of having only pairs with opposite momentum). An effective group velocity can be defined from Eq. (30) as

$$v_{k,j}^{\text{eff}}(p) = \sin \phi_k - \sin \left( \phi_k - \frac{2\pi j}{p} \right); \quad (31)$$

whose maximum value (over  $j$  and  $k$ ) is then the light-cone velocity

$$v_{\max} = \begin{cases} 2 & \text{when } p \text{ is even,} \\ 2 \cos\left(\frac{\pi}{2p}\right) & \text{when } p \text{ is odd.} \end{cases} \quad (32)$$

Eq. (32) predicts quantitatively the light-cone velocity of the signal (8) for the free fermion case. Note that the effective maximum group velocity occurs when  $j = \frac{p}{2}$  and  $j = \frac{p-1}{2}$  for even and odd  $p$ , respectively. In particular, from Eq. (32) follows that the actual light-cone velocity is state-dependent and cannot be faster than the maximum group velocity  $v_g$ . The prediction in Eq. (32) is in agreement with a numerical estimation of  $v_{\max}$ , obtained from the inflection points of the correlations  $\Delta_{ln}$ ; see Fig. 1 for examples with states labeled by  $(1/2, 1)$ ,  $(1/3, 1)$  and  $(1/2, 2)$ . It is also interesting to observe that the absolute minimum visible in the second and third panel in Fig. 1 is a finite size effect, indeed the envelope of  $|\Delta_{ln}(t)|$  is monotonically decreasing in the limit  $L \rightarrow \infty$  after reaching the first maximum.

A similar analysis for the initial states  $(s/p, s)$ , shows that

$$C_{ln} = \delta_{ln} - \frac{1}{Lp} \sum_{j=0}^{p-1} A_{js} e^{-\frac{2\pi i n j}{p}} \sum_{k=1}^L e^{-i[\phi_k(l-n) + 2t\varepsilon_{k,j}^{\text{eff}}(p)]} \quad (33)$$

where  $A_{js} = \sum_{q=0}^{s-1} e^{-\frac{2\pi i j q}{p}}$ . It is clear that as long as  $A_{js} \neq 0$  for the values of  $j$  corresponding to the effective maximum group velocity, Eq. (32) remains valid. However, one can verify that  $A_{js}$  is actually zero in some cases. For example, for the state labeled by  $(1/2, 2)$ , we have  $A_{22} = 0$  and therefore the light-cone velocity is obtained from the maximum over of Eq. (31) at  $j = 1$  and  $p = 4$ ; namely  $v_{\max} = \sqrt{2}$ . This is nicely confirmed in Fig. 1 (green curves).

### B. Arbitrary values of $\gamma$ and $h$ : Quenches from the Néel state ( $p = 2$ )

We start our analysis of the light-cone velocity for arbitrary values of  $\gamma$  and  $h$  in the XY chain from the neatest case of a quench from the Néel state; i.e.  $p = 2$  according to the notations of Sec. II. First observe that, for arbitrary values of  $\gamma$  and  $h$ , each term in the sum over  $j$  in Eqs. (25)-(26) is associated to a time propagation with an effective dispersion

$$\varepsilon_{k,j,\pm}^{\text{eff}}(p) = \frac{1}{2} \left( \varepsilon_k \pm \varepsilon_{\frac{L}{2}-k} \right), \quad j = 0, \dots, p-1, \quad (34)$$

where it is understood that for  $j = 0$  we get back Eq. (6). Moreover, also the first line in Eqs. (25)-(26) contains a state-independent contribution whose time evolution expands over the usual dispersion. Therefore as long as  $\gamma \neq 0$ , one should expect a state-independent light-cone

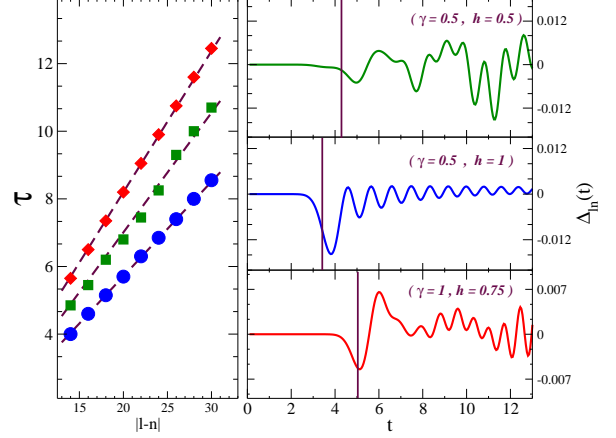


FIG. 2. (color online) On the right panel,  $\Delta_{ln}(t)$  for the XY chain and  $J = 1$  starting from the state  $(1/2, 1)$  with vertical bars in correspondence of  $\frac{|l-n|}{2v_{\max}}$ ; here  $L = 96$  and  $|l-n| = 12$ . On the left panel we plotted the numerically estimated inflection points  $\tau$  of the signals as a function of the distances  $|l-n|$ . The points align on a straight line with slope obtained from Eq. (35).

velocity  $v_{\max} = v_g$  (the maximum group velocity) for all the functions (9)-(10). However, as we already noticed at the end of Sec. III, for  $p = 2$  a propagation with the maximum group velocity  $v_g$  is forbidden by Eq. (27). For arbitrary values of the parameters  $\gamma$  and  $h$ , the effective maximum group velocity (i.e. the light-cone velocity) can be then obtained from Eq. (34) as

$$v_{\max} = \max_{j \neq 0, \pm, k} \frac{d\varepsilon_{k,j \neq 0, \pm}^{\text{eff}}(p)}{dk}. \quad (35)$$

Actually if  $p = 2$ , only  $j = 1$  is allowed in the formula above and as an immediate consequence  $v_{\max} < v_g$ ; Eq. (35) predicts the light-cone velocity of the signal (8) after a quench from the Néel state in the XY chain.

The physical interpretation is similar to the free fermion case: here the initial state allows only pairs of quasi-particles to propagate with momenta  $k$  and  $\frac{L}{2} - k$ . Notice also that the velocities of the pair are now different since  $|v_k| \neq |v_{\frac{L}{2}-k}|$  for  $v_k$  as in Eq. (7); this asymmetry diminishes the light-cone velocity. In the Ising chain ( $\gamma = 1$ )  $v_{\max}$  is obtained selecting the negative sign in Eq. (35), and  $\phi_k$  as close as possible to  $\frac{\pi}{2}$ . The explicit value is

$$v_{\max} = \frac{2Jh}{\sqrt{1+h^2}}. \quad (36)$$

Similarly, in the regions of the parameters  $h = 1$  and  $\gamma < \gamma^*$ , one finds

$$v_{\max} = \frac{2J}{\sqrt{1+\gamma^2}}; \quad (37)$$

where  $\gamma^*$  is the solution of  $\gamma^* = \frac{1}{\sqrt{1+(\gamma^*)^2}}$ . In general, there is not a closed formula for  $v_{\max}$ ; see however the

first and second panel in Fig. 6 for numerical estimations based on Eq. (35). In Fig. 2, we plot  $\Delta_{ln}(t)$  for different values of  $\gamma$  and  $h$  for quenches from the initial configuration  $(1/2, 1)$ . The light-cone velocities estimated from the inflection points are in agreement with Eqs. (36)-(37) and more generally with Eq. (35).

### C. Arbitrary values of $\gamma$ and $h$ : Quenches from states with $p > 2$

For  $p > 2$ , the determination of  $v_{\max}$  is considerably more involved and we cannot provide explicit formulas covering all the cases. To understand the source of new subtleties let us focus first on the critical Ising chain. Since for  $p > 2$  the terms in the first line of Eqs. (25)-(26) are not canceled, we should expect that the  $\mathbf{C}$  and  $\mathbf{F}$  matrix elements will propagate with a state-independent velocity  $v_g$ . This is indeed correct, see for instance the red and blue curves in the two panels of Fig. 3 with initial states  $p = 3$  and  $p = 4$ . However, when combined into  $\Delta_{ln}$ , the two signals almost exactly cancel around the first maximum, leaving a light-cone velocity slower than  $v_g$ . The latter can be still calculated as in case  $p = 2$  from Eq. (35). See the green curve in Fig. 3 for an illustration. This result holds also for any  $h \leq 1$  (ferromagnetic phase) as we support analytically in the Sec. V. For  $h > 1$  (paramagnetic phase), the same Sec. V shows instead that the correlation function  $\Delta_{ln}$  propagates with the maximum group velocity  $v_g$ . Summarizing for  $p > 2$ , in the Ising chain the signal in Eq. (8) propagates with a light cone velocity given by Eq. (35) for  $h \leq 1$  and by the maximum group velocity  $v_g$  for  $h > 1$ . This difference in the light-cone velocity between the two phases is hard to spot numerically, since the state-independent term is of order  $1/h^2$  and the difference between Eq. (35) and  $v_g$  drops to zero fast as  $h$  increases.

We studied the correlation function  $\Delta_{ln}$  for several different values of the parameters  $\gamma$  and  $h$ . For the initial states  $(\frac{1}{p}, 1)$  with  $p > 2$  we found numerically, similarly to the Ising chain,  $v_{\max}$  always to be given by Eq. (35) or  $v_g$ . However a clear pattern does not emerge from the numerical analysis and to distinguish between the two cases one should resort to the method described in Sec. V. For the configuration  $(1/2, 2)$  with  $p = 4$  again the terms that are independent from the initial states cancel out explicitly. For instance in the Ising chain the light-cone velocity is

$$v_{\max} = \frac{\sqrt{2}Jh}{\sqrt{1 - \sqrt{2}h + h^2}}; \quad (38)$$

a result that can be verified numerically from the inflection points. Similar arguments are also valid for all the configurations with  $(s/p, s)$ .

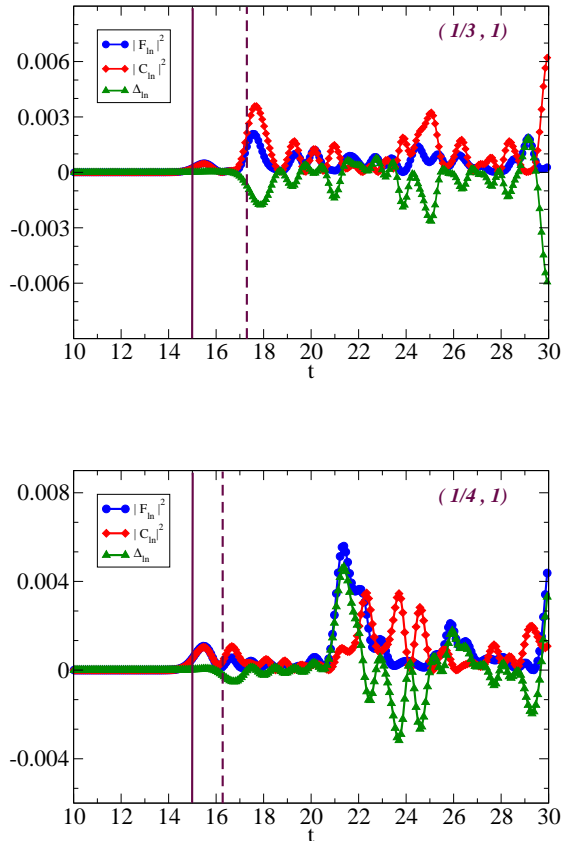


FIG. 3. (color online)  $|C_{ln}|^2$ ,  $|F_{ln}|^2$ , and  $\Delta_{ln}(t)$  for the XY chain with  $J = 1$ ,  $\gamma = 1$  and  $h = 1$  (critical Ising chain). The continuous vertical lines intersecting the red and blue curves are indicating the inflection points  $\tau$ . The dashed vertical line is in correspondence of the inflection point of  $\Delta_{ln}$  (green curve). It can be seen that  $|F_{ln}|$  and  $|C_{ln}|$  propagates faster than  $\Delta_{ln}$ . Here  $L = 144$  and  $|l - n| = 60$ .

## V. AIRY SCALING OF CORRELATION FUNCTIONS IN INFINITE VOLUME

In this section we describe how it is possible to obtain accurate approximations of the free fermionic correlation functions near the edge of the light cone in terms of combinations of Airy functions. The appearance of the Airy function at the boundary of the light-cone is not a novelty in the quench context, see<sup>24,25</sup> and also<sup>63,64</sup>. It is actually a direct consequence of stationary phase approximation in presence of coalescing stationary points; for more details and possible sources of violation of this approximation, see the comments below Eq. (54).

We start by determining the infinite volume limit ( $L \rightarrow \infty$ ) of the fermionic propagator and recast the results in Sec. III directly in Fourier space. We consider then fermionic operators  $c_l$  and  $c_n^\dagger$  with  $\{c_l^\dagger, c_n\} = \delta_{ln}$ ,  $\{c_l, c_n\} = \{c_l^\dagger, c_n^\dagger\} = 0$  defined for any  $l, n \in \mathbb{Z}$ . The

convention for the Fourier transforms are

$$c_l = \int_{-\pi}^{\pi} \frac{dk}{\sqrt{2\pi}} e^{ikl} c(k), \quad c(k) = \frac{1}{\sqrt{2\pi}} \sum_{l \in \mathbb{Z}} e^{-ikl} c_l, \quad (39)$$

from which follows that  $\{c^\dagger(k), c(k')\} = \delta(k - k')$  and  $\{c(k), c(k')\} = \{c^\dagger(k), c^\dagger(k')\} = 0$ . To be definite we only consider initial configurations labeled by the pair  $(1/p, 1)$ . In the XY chain, the time evolved operators  $c(-k, t)$  and  $c^\dagger(k, t)$  are linearly related to the correspondent operators at time zero. Indeed the Bogoliubov rotation that diagonalizes the XY chain is<sup>58</sup>

$$\begin{pmatrix} b^\dagger(k) \\ b(-k) \end{pmatrix} = \overbrace{\begin{pmatrix} \cos(\theta(k)/2) & -i \sin(\theta(k)/2) \\ -i \sin(\theta(k)/2) & \cos(\theta(k)/2) \end{pmatrix}}^{\mathcal{R}(k)} \begin{pmatrix} c^\dagger(k) \\ c(-k) \end{pmatrix} \quad (40)$$

with  $\cos \theta(k) = \frac{2J(\cos(k) - h/J)}{\varepsilon(k)}$ ,  $\sin \theta(k) = \frac{2J\gamma \sin(k)}{\varepsilon(k)}$  and  $\varepsilon(k) = 2J\sqrt{(\cos(k) - h/J)^2 + \gamma^2 \sin^2(k)}$ . The Bogoliubov fermions  $b(k)$  and  $b^\dagger(-k)$  have simple time evolution

$$\begin{pmatrix} b^\dagger(k, t) \\ b(-k, t) \end{pmatrix} = \overbrace{\begin{pmatrix} e^{i\varepsilon(k)t} & 0 \\ 0 & e^{-i\varepsilon(k)t} \end{pmatrix}}^{\mathcal{U}(k, t)} \begin{pmatrix} b^\dagger(k) \\ b(-k) \end{pmatrix} \quad (41)$$

and therefore we obtain

$$\begin{pmatrix} c^\dagger(k, t) \\ c(-k, t) \end{pmatrix} = \overbrace{\mathcal{R}^\dagger(k) \mathcal{U}(k, t) \mathcal{R}(k)}^{\tilde{T}(k, t)} \begin{pmatrix} c^\dagger(k) \\ c(-k) \end{pmatrix}. \quad (42)$$

The matrix elements of  $\tilde{T}$  are

$$\tilde{T}_{11}(k, t) = \cos(\varepsilon(k)t) + i \cos(\theta(k)) \sin(\varepsilon(k)t) \quad (43)$$

$$\tilde{T}_{12}(k, t) = \sin(\varepsilon(k)t) \sin(\theta(k)). \quad (44)$$

and  $\tilde{T}_{11}(k, t) = [\tilde{T}_{22}^*(k, t)]$ ,  $\tilde{T}_{21}(k, t) = -\tilde{T}_{12}(k, t)$ . From unitarity it follows moreover  $|\tilde{T}_{11}|^2 + \tilde{T}_{12}^2 = 1$  and  $\tilde{T}_{11}^* \tilde{T}_{12} + \tilde{T}_{21}^* \tilde{T}_{22} = 0$ . Fermionic correlation functions are double integrals in Fourier space. For instance let us denote by  $f^\alpha$  a fermionic operator with  $f^+ \equiv c$  and  $f^- \equiv c^\dagger$ , from the definition of the Fourier transform (39) we have

$$\langle f_t^\alpha(t) f_n^\beta(t) \rangle = \int \int \frac{dk dk'}{2\pi} e^{i\alpha k l + i\beta k' n} \langle f^\alpha(k, t) f^\beta(k', t) \rangle, \quad (45)$$

with integrals in the domain  $k, k' \in [-\pi, \pi]$ . The time evolution of the matrix element in (45) is obtained from Eq. (42) as a linear combination of four matrix elements of the same type at time  $t = 0$ . Among those four the only non-trivial on the class of initial states we are considering is  $g(k, k') = \langle c^\dagger(k) c(k') \rangle$ . Notice indeed that  $\langle c^\dagger(k) c^\dagger(k') \rangle = \langle c^\dagger(k) c^\dagger(k') \rangle = 0$  and  $\langle c(k) c^\dagger(k') \rangle$  can be obtained from the anticommutation relations. For our

initial state  $(\frac{1}{p}, 1)$  the function  $g$  is given by

$$g(k, k') = \frac{1}{2\pi} \sum_{n \in \mathbb{Z}} e^{inp(k-k')} = \frac{1}{p} \sum_{j=0}^{p-1} \delta\left(k - k' - \frac{2\pi j}{p}\right). \quad (46)$$

It is then straightforward to derive integral representations for the correlators  $F_{ln}(t)$  and  $C_{ln}(t)$  that we write as

$$F_{ln}(t) = \sum_{j=0}^{p-1} F_{ln}^j(t) \quad \text{and} \quad C_{ln}(t) = \sum_{j=0}^{p-1} C_{ln}^j(t). \quad (47)$$

Explicit expressions for the functions  $F_{ln}^j(t)$  and  $C_{ln}^j(t)$  are

$$F_{ln}^0(t) = \int \frac{dk}{2\pi} e^{-ik(l-n)} \left[ \tilde{T}_{12}(k, t) \tilde{T}_{11}(-k, t) + \frac{1}{p} (\tilde{T}_{11}(k, t) \tilde{T}_{12}(-k, t) - \tilde{T}_{12}(k, t) \tilde{T}_{11}(-k, t)) \right], \quad (48)$$

$$F_{ln}^{j \neq 0}(t) = \frac{e^{-\frac{2\pi i n j}{p}}}{p} \int \frac{dk}{2\pi} e^{-ik(l-n)} \left[ \tilde{T}_{11}(k, t) \times \right. \\ \left. \times \tilde{T}_{12}\left(-k + \frac{2\pi j}{p}, t\right) - \tilde{T}_{12}(k, t) \tilde{T}_{11}\left(-k + \frac{2\pi j}{p}, t\right) \right]; \quad (49)$$

and analogously

$$C_{ln}^0(t) = \int \frac{dk}{2\pi} e^{ik(l-n)} \left[ \tilde{T}_{22}(-k, t) \tilde{T}_{11}(k, t) \left(1 - \frac{1}{p}\right) + \frac{1}{p} \tilde{T}_{12}(k, t)^2 \right], \quad (50)$$

$$C_{ln}^{j \neq 0}(t) = \frac{e^{-\frac{2\pi i n j}{p}}}{p} \int \frac{dk}{2\pi} e^{ik(l-n)} \left[ \tilde{T}_{21}(-k, t) \times \right. \\ \left. \times \tilde{T}_{12}\left(k + \frac{2\pi j}{p}, t\right) - \tilde{T}_{22}(-k, t) \tilde{T}_{11}\left(k + \frac{2\pi j}{p}, t\right) \right]. \quad (51)$$

Notice that the integrals in Eqs. (48) and (50) are of course the  $L \rightarrow \infty$  limit of Eqs. (25)-(26). Each function  $F_{ln}^j(t)$  and  $C_{ln}^j(t)$  describes a time propagation with a velocity that can be derived from the effective dispersion relation

$$\varepsilon_{j, \pm}^{\text{eff}}(k, p) = \frac{1}{2} \left[ \varepsilon(k) \pm \varepsilon\left(-k + \frac{2\pi j}{p}\right) \right], \quad j = 0, \dots, p-1, \quad (52)$$

that is Eq. (34) in the limit  $L \rightarrow \infty$ . As in Sec. III, the prediction of the light-cone velocity follows from calculating the maximum effective group velocities obtained from Eq. (52). In particular, it can be easily verified (see Eqs. (48) and (50) in particular) that for  $p = 2$ , the maximum effective group velocity is always smaller than  $v_g$  obtained from Eq. (7).

As shown in Fig. 3, the numerics indicates that a cancellation of the fastest  $j = 0$  contributions in Eq. (52) appears also for  $p \neq 2$  in the critical Ising chain. This observation extends to the whole ferromagnetic phase  $h \leq 1$ . It can be understood analytically comparing the behaviors near their inflection points of  $|F_{ln}^0(t)|$  and  $|C_{ln}^0(t)|$  in (47) and showing that they are the same. At the edge of the light-cone those functions can indeed be approximated by an Airy function with increasing accuracy as  $t \rightarrow \infty$  as we now discuss.

Consider an integral of the form

$$I(x, t) = \int_{-\pi}^{\pi} \frac{dk}{2\pi} H(k) e^{2it\varepsilon(k) - ikx} \quad (53)$$

where we assume  $x > 0$  and  $H(k)$  a function with support into  $[-\pi, \pi]$ . We consider the asymptotic of such an integral for large  $t$ , keeping fixed the ratio  $x/t$ . The boundary of the light-cone is identified by the condition that the solution  $k_{\max}$  of the stationary phase equation

$$\varepsilon'(k_{\max}) = \frac{x}{2t}, \quad (54)$$

corresponds to a point of maximum of the function  $\varepsilon'(k)$ . There are then two possibilities: either  $\varepsilon''(k_{\max}) = 0$  or  $\varepsilon''(k_{\max}) \neq 0$ . The latter case can happen for instance if  $k_{\max}$  lies at the boundary of the integration domain. The Airy scaling is obtained when  $\varepsilon''(k_{\max}) = 0$  and in a Taylor expansion of the phase near  $k = k_{\max}$  the third order term is not zero (for instance<sup>25,63,64</sup>). If  $H(k_{\max}) \neq 0$ , it is easy to obtain the following approximation of the integral  $I(x, t)$  near the boundary of the light-cone

$$I(x, t) \simeq \frac{e^{2it\varepsilon(k_{\max}) - ik_{\max}x} H(k_{\max})}{[-t\varepsilon'''(k_{\max})]^{1/3}} \text{Ai}(-X), \quad (55)$$

being  $X = \frac{2\varepsilon'(k_{\max})t - x}{[-t\varepsilon'''(k_{\max})]^{1/3}}$  and  $\text{Ai}(x) = \int_{-\infty}^{\infty} \frac{dq}{2\pi} e^{iqx + \frac{iq^3}{3}}$ . It should be noticed that (55) is determined in the limit  $t \rightarrow \infty$  but it gives a fairly good approximation of the integral as long as

$$|2\varepsilon'(k_{\max})t - x| \ll [-t\varepsilon'''(k_{\max})]^{1/3}. \quad (56)$$

Let us now pass to illustrate a concrete application of Eq. (55) to the Ising chain where we fixed  $J = 1/2$  and  $\gamma = 1$ . The functions  $F_{ln}^0(t)$  and  $C_x^0(t)$  can be written as

$$F_{ln}^0(t) = H_0 + \sum_{\sigma=\pm} \int_{-\pi}^{\pi} \frac{dk}{2\pi} H_{\sigma}(k) e^{2i\sigma\varepsilon(k)t - ik(l-n)}, \quad (57)$$

$$C_{ln}^0(t) = K_0 + \sum_{\sigma=\pm} \int_{-\pi}^{\pi} \frac{dk}{2\pi} K_{\sigma}(k) e^{2i\sigma\varepsilon(k)t - ik(l-n)}; \quad (58)$$

where  $H_{\pm}$  and  $K_{\pm}$  are obtained expanding the integrands in (48) and (50) and we also used  $C_{ln}^0(t) = C_{nl}^0(t)$ . The constant terms  $H_0$  and  $K_0$  can be also determined explicitly from the residue theorem and they are given by

$$H_0 = K_0 = -\frac{h^{x-2}(h^2 - 1)(p - 2)}{8p}, \quad h \leq 1; \quad (59)$$

$$H_0 = -K_0 = -\frac{h^{-x+2}(h^2 - 1)(p - 2)}{8p}, \quad h > 1, \quad (60)$$

where we defined  $x \equiv (l - n) \geq 2$ . They are then vanishing at  $h = 1$  or are exponentially small with the distance  $x$  when  $h \neq 1$ . Since we will consider only large values of  $x$ , it turns out that they are negligible.

We focus first on the case  $h < 1$ . Here we have  $k_{\max} = \arccos(h)$ ,  $\varepsilon'(k_{\max}) \equiv v_g = h$ ,  $\varepsilon''(k_{\max}) = 0$ ,  $\varepsilon'''(k_{\max}) = -h$ ; using (55) we obtain for  $t \rightarrow \infty$  the light-cone approximations

$$F_{ln}^0(t) \simeq \frac{2H_+(k_{\max}) \cos[2th\phi(h)]}{(ht)^{1/3}} \text{Ai}(X) \quad (61)$$

$$C_{ln}^0(t) \simeq \frac{2K_+(k_{\max}) \cos[2th\phi(h)]}{(ht)^{1/3}} \text{Ai}(X). \quad (62)$$

where  $\phi(h) = \sqrt{1/h^2 - 1} - \arccos(h)$ . It turns out that  $H_+(k_{\max}) = H_-(-k_{\max}) = -iK_+(k_{\max}) = -iK_-(-k_{\max})$  and

$$H_+(k_{\max}) = -i\frac{p-2}{4p}, \quad (63)$$

Therefore  $|F_{ln}^0|^2$  and  $|C_{ln}^0|^2$  have the same approximation in terms of an Airy function and they cancel out when calculating  $\Delta_{ln}$ .

We now pass to discuss the case  $h > 1$ . Here we have  $k_{\max} = \arccos(1/h)$ ,  $\varepsilon'(k_{\max}) \equiv v_g = 1$ ,  $\varepsilon''(k_{\max}) = 0$ ,  $\varepsilon'''(k_{\max}) = -1$ . A similar expansion gives the approximations

$$F_{ln}^0(t) \simeq \frac{e^{2it\phi(h^{-1})} H_+(k_{\max}) + e^{-2it\phi(h^{-1})} H_-(-k_{\max})}{t^{1/3}} \text{Ai}(X) \quad (64)$$

$$C_{ln}^0(t) \simeq \frac{2K_+(k_{\max}) \cos[2t\phi(h^{-1})]}{t^{1/3}} \text{Ai}(X), \quad (65)$$

where now  $K_+(k_{\max}) = K_-(-k_{\max})$  and

$$H_{\pm}(\pm k_{\max}) = -i\frac{(h \mp \sqrt{h^2 - 1})(p - 2)}{4h^2p} \quad (66)$$

$$K_+(k_{\max}) = \frac{p-2}{4h^2p}. \quad (67)$$

There is no more a cancellation of the two terms as for  $h < 1$ . The absence of a clear peak at  $\tau = \frac{l-n}{2}$  ( $l \gg n$ ) in the observable  $\Delta_{ln}(t)$  that emerges in the numerics can be however understood as a combination of three effects. For large  $h \gg 1$ , the values at the inclination point of  $|F_{ln}^0|^2$  and  $|C_{ln}^0|^2$  are suppressed by a factor  $1/h^2$  and  $1/h^4$  respectively and moreover the difference between Eq. (35) and  $v_g$  is small. On the other hand, as  $h \rightarrow 1$ , an exact cancellation between  $|F_{ln}^0|$  and  $|C_{ln}^0|$  must happen.

For  $h = 1$ , the two distinct stationary points  $\pm k_{\max}$  actually merge at  $k = 0$  and the asymptotic expansion involves only one term. One has  $v_g = 1$  and  $\varepsilon''(0^+) = 0$ ,  $\varepsilon'''(0^+) = -1/4$ ; leading to the final result

$$F_{ln}^0(t) \simeq -i\frac{p-2}{2p(2t)^{1/3}} \text{Ai}(X), \quad C_{ln}^0(t) = -iF_{ln}^0(\tau), \quad (68)$$



that once again shows the cancellation of the fastest particle contribution for arbitrary values of  $p$ . Although the argument applies for large  $t$ , we believe that it furnishes a satisfactory explanation of the numerical results presented in Fig. 3. Finally notice that the limits  $h \rightarrow 1^\pm$ , although producing the same result, do not commute with the asymptotic expansion.

Analogous approximations could be calculated for all the functions  $F_{ln}^j(t)$  and  $C_{ln}^j(t)$  with the same technique. As a last example, we demonstrate the validity of the Airy-approximation, through the neatest example of a quench from the Néel state ( $p = 2$ ) in the critical Ising chain. In this case the integrals  $F_{ln}^0(t)$  and  $C_{ln}^0(t)$  vanish for any time. For  $t \rightarrow \infty$  and  $x/t$  finite, being  $x \equiv l - n > 0$ ; we obtain

$$(4t)^{2/3} \Delta_{ln}(t) \simeq -\text{Ai}^2(-X), \quad t \gg 1. \quad (69)$$

In (69),  $X = \frac{2v_{\max}t-x}{[-te'''(k_{\max})]^{1/3}} \in \mathbb{R}$ ,  $k_{\max} = \pi/2$  and according to (52)

$$e(k) \equiv \varepsilon_{1,-}^{\text{eff}}(k, 2) = \frac{1}{2}[\varepsilon(k) - \varepsilon(-k + \pi)] \quad (70)$$

$$v_{\max} = \max_{k \in [-\pi, \pi]} \frac{de(k)}{dk} = \frac{1}{\sqrt{2}}. \quad (71)$$

The value of  $v_{\max}$  is of course the same as in Eq. (35) taking  $J = 1/2$ . A comparison of the stationary phase approximation in Eq. (69) with a numerical evaluation of the correlation function  $\Delta_{ln}(t)$  is presented in Fig. 4. It is finally worth to remark that for  $X = 0$  (i.e.  $t = \frac{|l-n|}{2v_{\max}}$ ), Eq. (69) is within the 10% from the exact value already for  $t = 50$ . Notice also that  $\text{Ai}''(0) = 0$  which explains why for large times the inflection point of the signal is close to  $\frac{|l-n|}{2v_{\max}}$ .

## VI. EVOLUTION OF THE ENTANGLEMENT ENTROPY

In this final section before the conclusions, we present numerical results for the time evolution of the entanglement entropy of a subsystem of size  $l$  for the different initial states discussed in Sec. II. Based on a quasi-particle picture<sup>46,47</sup>, we expect the entanglement entropy, denoted by  $S(t)$ , to grow linearly in time up to  $\tau_s$  which is approximately  $\frac{l}{2v_g}$ . After  $\tau_s$ , which we will call the saturation time, the entanglement entropy converges<sup>48</sup> to the von Neumann entropy of the stationary state<sup>52,65</sup>. In the numerics  $\tau_s$  is obtained as the earliest time where the second derivative of the signal changes.

One can calculate the entanglement entropy from the correlation functions as follows<sup>62</sup>

$$S = -\text{Tr} \left[ \frac{1+\mathbf{\Gamma}}{2} \ln \left( \frac{1+\mathbf{\Gamma}}{2} \right) \right], \quad (72)$$

where  $\mathbf{\Gamma}$  is a  $2l \times 2l$  block matrix which can be written

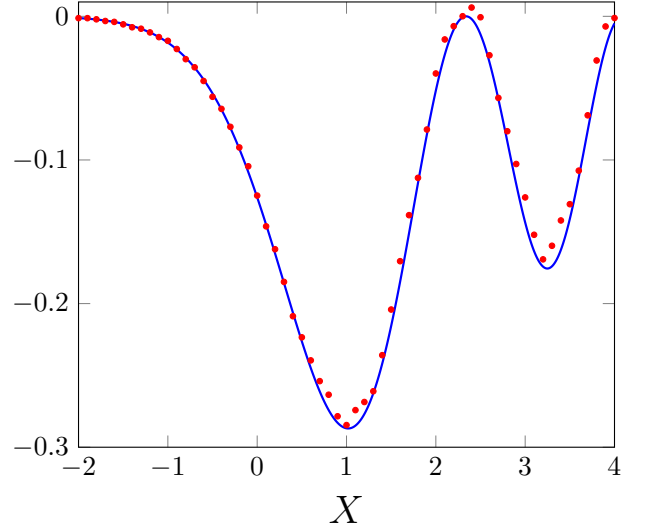


FIG. 4. The continuous blue curve is the function  $-\text{Ai}^2(-X)$ . The points represent numerical evaluations of  $(4t)^{2/3} \Delta_{ln}(t)$  for a quench from the Néel state ( $p = 2$ ) in the critical Ising chain ( $h = \gamma = 1$  and  $J = 1/2$ ). Here  $|l - n| = 2v_{\max}t - [-te'''(k_{\max})]^{1/3}X$  and  $t = 500$ .

as

$$\begin{aligned} \mathbf{\Gamma}_{mn} &= \left\langle \begin{pmatrix} a_m^x \\ a_m^y \end{pmatrix} \begin{pmatrix} a_n^x & a_n^y \end{pmatrix} \right\rangle - \delta_{mn} \mathbf{1}_{2 \times 2} \\ &= \begin{pmatrix} \langle a_m^x a_n^x \rangle - \delta_{mn} & \langle a_m^x a_n^y \rangle \\ \langle a_m^y a_n^x \rangle & \langle a_m^y a_n^y \rangle - \delta_{mn} \end{pmatrix}. \end{aligned} \quad (73)$$

Here  $a_m^x = c_m^\dagger + c_m$  and  $a_m^y = i(c_m - c_m^\dagger)$  and the indexes  $m, n$  belong to the one-dimensional subsystem of size  $l$ . One can easily find all the different elements of the matrix  $\mathbf{\Gamma}$  as,

$$\mathbf{\Gamma}_{11} = \mathbf{F} + \mathbf{F}^\dagger + \mathbf{C} - \mathbf{C}^T, \quad (74)$$

$$\mathbf{\Gamma}_{12} = i(\mathbf{1} - \mathbf{C} - \mathbf{C}^T - \mathbf{F} + \mathbf{F}^\dagger), \quad (75)$$

$$\mathbf{\Gamma}_{21} = -i(\mathbf{1} - \mathbf{C} - \mathbf{C}^T + \mathbf{F} - \mathbf{F}^\dagger), \quad (76)$$

$$\mathbf{\Gamma}_{22} = -\mathbf{F} - \mathbf{F}^\dagger + \mathbf{C} - \mathbf{C}^T. \quad (77)$$

At this stage we have all the ingredients to build the matrix  $\mathbf{\Gamma}$  and consequently to calculate the entanglement entropy from Eq. (72). In fact, one can calculate the entanglement from

$$S = - \sum_{j=1}^l \left[ \frac{1+\nu_j}{2} \ln \left( \frac{1+\nu_j}{2} \right) + \frac{1-\nu_j}{2} \ln \left( \frac{1-\nu_j}{2} \right) \right], \quad (78)$$

where  $\nu_j$ 's are the positive eigenvalues of the matrix  $\mathbf{\Gamma}$ .

Let us now pass to summarize the numerical results illustrated in Fig. 5a and Fig. 5b. Firstly, it is evident that, as long as  $p > 1$  and  $\gamma \neq 0$ ,  $v_g$  does not necessarily play a role into the time evolution of the entanglement

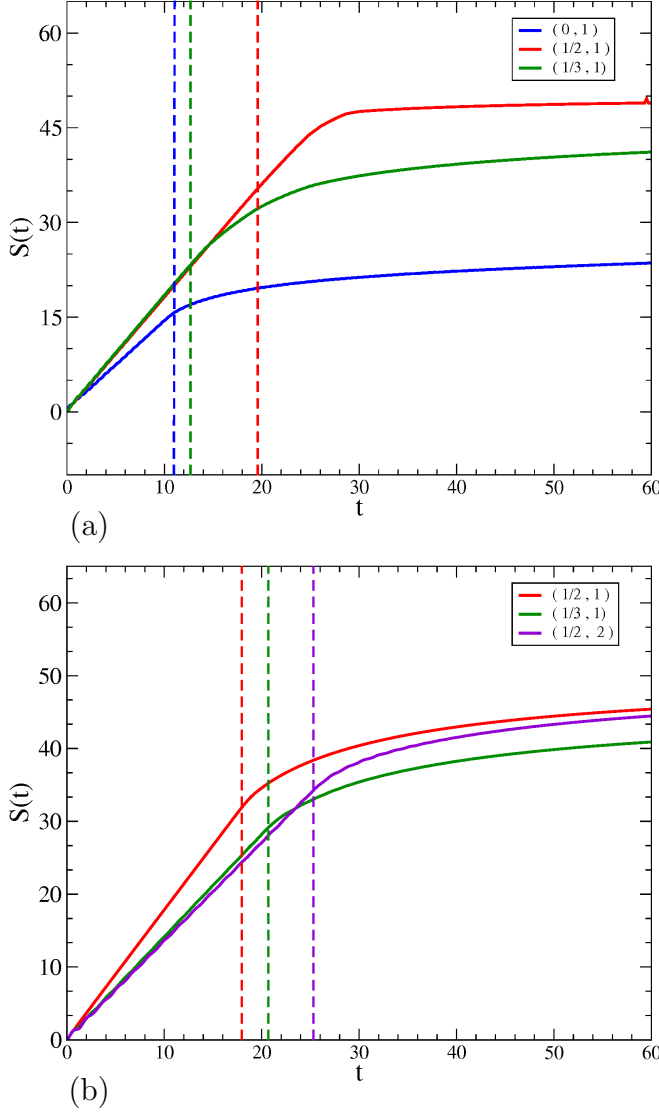


FIG. 5. (color online) The evolution of the entanglement entropy in the XY chain with system size  $L = 600$  and  $l = 72$ . The vertical dashed lines are in correspondence of  $t = \frac{l}{2v_{\max}}$ , being  $v_{\max}$  the light-cone velocity for the correlation functions obtained in Sec. IV. (a)  $S(t)$  at  $\gamma = 2$  and  $h = 1.5$ . The blue curve corresponds to time evolution from  $p = 1$  (i.e. a fully polarized initial state) and the green one to  $p = 3$ . Both are compatible with  $\tau_s = \frac{l}{2v_{\max}}$ , notice that for  $p = 1$   $v_{\max} = v_g$ . The red curve corresponds instead to  $p = 2$  and shows that in such a case the saturation time is larger than  $\frac{l}{2v_{\max}}$ . (b)  $S(t)$  in the free fermion case  $\gamma = h = 0$  and  $J = -1$ , here the saturation time is in agreement with the conjecture  $\tau_s = \frac{l}{2v_{\max}}$ .

entropy. See Fig. 5a and compare the blue curve, corresponding to  $S(t)$  for  $p = 1$  (i.e. a fully polarized initial state  $|\psi_0\rangle = |\uparrow\uparrow\ldots\uparrow\rangle$ ) with the green that refers instead to  $p = 3$ ; in both cases  $\gamma = 2$  and  $h = 1.5$ . It is clear that starting from an initial state with  $p \neq 1$ , the saturation time is state-dependent and larger than  $\frac{l}{2v_g}$ .

Mimicing the original interpretation in<sup>46,47</sup>, it is

tempting to conjecture that  $\tau_s$  could be approximated instead by  $\frac{l}{2v_{\max}}$ , with  $v_{\max}$  the light-cone velocity extracted from the correlation functions in Sec. III. This natural conjecture can be readily verified, for instance, in the free fermion case  $\gamma = h = 0$  and  $J = -1$ . In Fig. 5b we report numerical simulations at  $\gamma = h = 0$  and  $J = -1$  for  $S(t)$  starting different initial states. From top to bottom the configurations that label the selected initial states are  $(1/p, 1)$ , with  $p = 2, 3$  and  $(1/2, 2)$ . In the free fermion case the saturation time is then fully compatible with the conjecture  $\tau_s = \frac{l}{2v_{\max}}$  and  $v_{\max}$  given in Eq. (32) and below Eq. (33). In particular, the agreement for the configuration  $(\frac{1}{2}, 2)$  is remarkable because the result  $v_{\max} = \sqrt{2}$  was derived in Sec. IV A by using  $A_{22} = 0$ .

We have done a similar analysis for several different values of  $\gamma$  and  $h$  to check whether the conjecture for  $\tau_s$  holds more generally in the XY chain. The final answer is negative as can be understood again from Fig. 5a, analyzing in particular the red and green curves. The green curve describes  $S(t)$  for  $p = 3$  ( $h = 1.5$  and  $\gamma = 2$ ) where  $v_{\max}$  is obtained from Eq. (35) and shows that the saturation time is again compatible with  $\frac{l}{2v_{\max}}$ . The red curve describes instead  $S(t)$  for  $p = 2$  ( $h = 1.5$  and  $\gamma = 2$ ) and according to the analysis in Sec. III, the light-cone velocity  $v_{\max}$  is again given by Eq. (35). However the entanglement entropy displays a saturation time larger than  $\frac{l}{2v_{\max}}$ . At present we do not have an analytical understanding of this effect. However, our numerical simulations indicate that  $v_{\max}$  sets a lower bound on the saturation time and actually  $\tau_s \geq \frac{l}{2v_{\max}}$ .

## VII. CONCLUSIONS

In this paper we have analyzed the influence of the initial state on the maximum speed at which correlations can propagate, according to the Lieb-Robinson bound. We investigated the XY chain and global quenches from a class of initial states that are factorized in the local  $z$ -component of the spin and have a crystalline structure. We demonstrated explicitly that momentum conservation in the crystal leads to a state-dependent light-cone velocity  $v_{\max}$  that rules how fast correlations spread. For instance, see Sec. IV B below Eq. (35), pairs of quasi-particles can travel after the quench with momenta that are no more opposite. This effect slows down the signal propagation.

We have given, and checked numerically, analytical predictions for the light-cone velocities for several values of the parameters  $\gamma$ ,  $h$  and  $p$ ; concrete examples are given in Eq. (32) and Eq. (35). We also discussed an approximation of the fermionic correlations functions in infinite volume that shows, in agreement with previous results in<sup>24,25</sup>, that the behaviour at the light-cone edge can be characterized by integer powers of  $t^{-1/3}$ . In particular this is the case when the light-cone velocity is a

maximum with vanishing second derivative (and non-zero third derivative) of the effective dispersion. The degree of universality of the  $t^{-1/3}$ -scaling and in particular its dependence on the initial state, however, have been not clarified yet<sup>66–70</sup>.

We have then studied numerically the evolution of the entanglement entropy and showed that the choice of the initial state affects also the saturation time. When completing this paper, a preprint<sup>71</sup> appeared that analyzes entanglement dynamics in the XX chain ( $\gamma = 0$ ) for the class of initial states here labeled as  $(1/p, 1)$ . In particular an interesting semiclassical interpretation in terms of entangled  $p$ -plets of quasi-particles is proposed. Our calculations in Sec. III for the light-cone velocity in the XX chain are in agreement with such a quasi-particle picture. It will be important to investigate how this can be adapted to determine the light-cone velocity  $v_{\max}$  and the linear growth of the entanglement entropy also for  $\gamma \neq 0$ . Our analysis suggests that these observables are not easily predictable on the whole parameters space, therefore a generalized quasi-particle picture will be likely initial state dependent. Finally, it will be relevant to study the effect of the initial state on Loschmidt echo and finite

size effects<sup>72,73</sup>.

**Acknowledgement** We are indebted to Pasquale Calabrese for important observations on the draft of this manuscript. The work of K.N. is supported by National Science Foundation under Grant No. PHY- 1314295. The work of MAR was supported in part by CNPq. JV and MAR thank the INCT-IQ initiative for partial support. JV also thanks LPTHE-Paris VI, SISSA and the University of Florence for their kind hospitality.

## Appendix A: Light-cone velocities for $p = 2$

As we discussed in the main part of the paper different initial states can induce different effective maximum group velocities. A fully translation invariant initial state with all the spins up or down ( $p = 1$ ) leads to a propagation with velocity  $v_g$ , the maximum of Eq. (7). However, for state  $(1/2, 1)$   $v_{\max}$  is fixed by Eq. (35) and can be easily found numerically. In Fig. 6 we plot the light-cone velocities for  $p = 2$  obtained in this way and compare them against  $v_g$ . The figure clearly shows that for small values of  $\gamma$  and  $h$  the difference between the two are negligible. A difference (denoted as  $d$  in Fig. 6) between the light-cone velocity and  $v_g$  is instead more pronounced close to  $h = 1$ . This will be the best condition to test the effects studied in this paper.

<sup>1</sup> E.H. Lieb and D. Robinson, Commun. Math. Phys. **28**, 251 (1972).

<sup>2</sup> S. Bravyi, M. B. Hastings and F. Verstraete. Phys. Rev. Lett. **97**, 050401 (2006).

<sup>3</sup> J. Eisert and T.J. Osborne, Phys. Rev. Lett **97**, 150404 (2006).

<sup>4</sup> B. Nachtergaele and R. Sims, Commun. Math. Phys. **265**, 119 (2006).

<sup>5</sup> The explicit form of the velocity can be written by first defining the form of the interaction. Consider a quantum spin system defined over a discrete set  $\Gamma$  with the Hamiltonian  $H_\Lambda = \sum_{X \subset \Lambda} \Phi(X)$ , where  $\Lambda \subset \Gamma$ . Suppose now a non-increasing function  $F : [0, \infty) \rightarrow (0, \infty)$  with the following properties  $\|F\| = \max_{x \in \Gamma} \sum_{y \in \Gamma} F(|x - y|) < \infty$  and  $C = \max_{x \in \Gamma} \sum_{z \in \Gamma} \frac{F(|x - z|)F(|z - y|)}{F(|x - y|)} < \infty$  and  $\|\Phi\| = \max_{x, y \in \Gamma} \frac{1}{F(|x - y|)} \sum_{\substack{X \subset \Gamma \\ x, y \in X}} \|\Phi(X)\| < \infty$ . Now for any non-

negative real  $\mu$  the  $F_\mu(x) = e^{-\mu x} F(x)$  has the same properties as  $F(x)$  and  $\|F\| \geq \|F_\mu\|$  and  $C \geq C_\mu$ . Then the LR velocity can be written as  $v_{LR} = \max_{\mu} \frac{2\|\Phi_\mu\|C_\mu}{\mu}$ .

<sup>6</sup> J. Eisert, M. Cramer, and M. B. Plenio Rev. Mod. Phys. **82**, 277 (2010).

<sup>7</sup> M. B. Hastings, J. Math. Phys. **50**, 095207 (2009).

<sup>8</sup> M. B. Hastings and T. Koma, Commun. Math. Phys. **265**, 781 (2006).

<sup>9</sup> B. Nachtergaele and R. Sims, IAMP News Bulletin, pp 22-29 (2010).

<sup>10</sup> T. Kinoshita, T. Wenger, and D. S. Weiss, Nature **440**, 900 (2006).

<sup>11</sup> S. Hofferberth, I. Lesanovsky, B. Fischer, T. Schumm, and J. Schmiedmayer, Nature **449**, 324 (2007).

<sup>12</sup> I. Bloch, J. Dalibard and W. Zwerger, Rev. Mod. Phys. **80**, 885 (2008).

<sup>13</sup> F. Meinert, M.J. Mark, E. Kirilov, K. Lauber, P. Weinmann, A.J. Daley and H-C. Nagerl, Phys. Rev. Lett. **111**, 053003 (2013).

<sup>14</sup> T. Langen, S. Erne, R. Geiger, B. Rauer, T. Schweigler, M. Kuhnert, W. Rohringer, I.E. Mazets, T. Gasenzer and J. Schmiedmayer, Science **348**, 6231 (2015).

<sup>15</sup> A. Polkovnikov, K. Sengupta, A. Silva, and M. Vengalattore, Rev. Mod. Phys. **83**, 863 (2011).

<sup>16</sup> C. Gogolin and J. Eisert, Reports on Progress in Physics **79** (5), 056001 (2016).

<sup>17</sup> L. Vidmar, M. Rigol, J. Stat. Mech. (2016) 064007

<sup>18</sup> P Calabrese, F. H. L. Essler, and G. Mussardo Introduction to J. Stat. Mech special issue “Quantum Integrability in Out of Equilibrium Systems” (2016) 064001.

<sup>19</sup> A. Lauchli and C. Kollath, J. Stat. Mech. (2008)P05018.

<sup>20</sup> S. Manmana, S. Wessel, R. Noack and A. Muramatsu, Phys. Rev. B **79** 155104 (2009).

<sup>21</sup> P. Calabrese, F. H. L. Essler and M. Fagotti, Phys. Rev. Lett. **106** 227203 (2011).

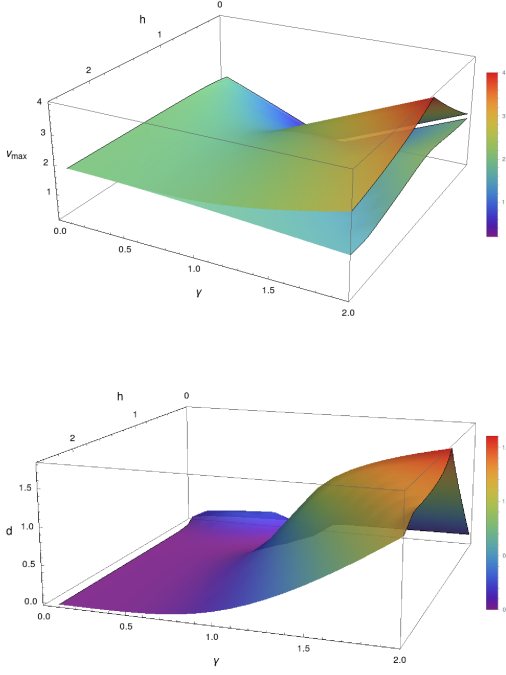


FIG. 6. (color online) From top to bottom. First panel: Maximum group velocity  $v_{\max}$ , obtained from Eq. (35) and  $v_g$  for different values of  $\gamma$  and  $h$  at  $p = 2$ . Second panel: The difference  $d$  between  $v_{\max}$  and  $v_g$  at  $p = 2$ . Here we took  $J = 1$ .

- 22 P. Calabrese, F. H. L. Essler and M. Fagotti, J. Stat. Mech. (2012)P07016.
- 23 P. Calabrese, F. H. L. Essler and M. Fagotti, J. Stat. Mech. (2012)P07022
- 24 P. Barmettler, D. Poletti, M. Cheneau, and C. Kollath Phys. Rev. A **85**, 053625 (2012).
- 25 B. Bertini, F. H. L. Essler, S. Groha, N. Robinson, Phys. Rev. B **94**, 245117 (2016).
- 26 J. Dubail, J-M. Stéphan, P. Calabrese, SciPost Phys. **3**, 019 (2017).
- 27 L. Cevolani, J. Despres, G. Carleo, L. Tagliacozzo, L. Sanchez-Palencia [arXiv:1706.00838]
- 28 S. Porta, F. M. Gambetta, F. Cavaliere, N. Traverso Ziani, and M. Sassetti, Phys. Rev. B **94**, 085122 (2016)
- 29 S. Porta, F. M. Gambetta, N. Traverso Ziani, D. M. Kennes, M. Sassetti, and F. Cavaliere, Phys. Rev. B **97**, 035433 (2018)
- 30 L. Bonnes, F. H. L. Essler, A. M. Lauchli, Phys. Rev. Lett. **113**, 187203 (2014).
- 31 G. Carleo, F. Becca, L. Sanchez-Palencia, S. Sorella and M. Fabrizio, Phys. Rev. A (R) **89**, 031602 (2014).
- 32 F. H. L. Essler and M. Fagotti, J. Stat. Mech. (2016) 064002.
- 33 P. Calabrese and J. Cardy, J. Stat. Mech. (2005) 0504:P04010.
- 34 G. De Chiara, S. Montangero, P. Calabrese and R. Fazio, J. Stat. Mech. (2006) P03001.
- 35 M. Fagotti and P. Calabrese, Phys. Rev. A **78**, 010306(R) (2008).
- 36 J-M. Stéphan and J. Dubail, J. Stat. Mech. (2011) P08019.
- 37 H. Kim and D. A. Huse, Phys. Rev. Lett. **111** 127205 (2013).
- 38 M. Ghasemi Nezhadhighi and M. A. Rajabpour, Phys. Rev. B **90**, 205438 (2014).
- 39 J. Dubail, J. Phys. A: Math. Theor. **50** 234001 (2017).
- 40 A. Nahum, J. Ruhman, S. Vijay, and J. Haah, Phys. Rev. X **7**, 031016 (2017).
- 41 C. Jonay, D. A. Huse and A. Nahum, [arXiv:1803.00089].
- 42 M. Cheneau, P. Barmettler, D. Poletti, M. Endres, P. Schauss, T. Fukuhara, C. Gross, I. Bloch, C. Kollath and S. Kuhr, Nature **481**, 484 (2012).
- 43 T. Langen, R. Geiger, M. Kunhert, B. Rauer and J. Schmiedmayer, Nature. Phys. **9** 640 (2013).
- 44 P. Richerme, Z.-X. Gong, A. Lee, C. Senko, J. Smith, M. Moss-Feig, S. Michalakakis, A. V. Gorshkov, and C. Monroe, Nature **511**, 198 (2014).
- 45 Jurcevic, B. P. Lanyon, P. Hauke, C. Hempel, P. Zoller, R. Blatt, and C. F. Roos, Nature **511**, 202 (2014).
- 46 P. Calabrese and J. Cardy, Phys. Rev. Lett **96** 136801 (2006).
- 47 P. Calabrese and J. Cardy, J. Stat. Mech. (2007) 0706:P06008.
- 48 V. Alba and P. Calabrese, PNAS **114**, 7947 (2017).
- 49 V. Alba and P. Calabrese, SciPost Phys. **4**, 017(2018).
- 50 C. Pascu Moca, M. Kormos, and G. Zarand, Phys. Rev. Lett. **119**, 100603 (2017)
- 51 G. Delfino, [arXiv:1710.06275].
- 52 J. S. Caux and F. H. L. Essler, Phys. Rev. Lett. **110**, 257203 (2013).
- 53 M. Rigol, V. Dunjko, V. Yurovsky and M. Olshanii, Phys. Rev. Lett. **98**, 050405 (2007).
- 54 M. Rigol, V. Dunjko and M. Olshanii Nature **452**, 854 (2008).
- 55 O. Castro-Alvaredo, B. Doyon and T. Yoshimiura, Phys. Rev. X **6**, 041065 (2016).
- 56 B. Bertini, M. Collura, J. De Nardis and M. Fagotti, Phys. Rev. Lett. **117**, 207201 (2016).
- 57 Vir B. Bulchandani, R. Vasseur, C. Karrasch and J. E. Moore, Phys. Rev. Lett. **119**, 220604 (2017).
- 58 E. Lieb, T. Schultz, and D. Mattis, Annals of Physics **16**, 407 (1961).
- 59 L. Bucciattini, M. Kormos, P. Calabrese, J. Phys. A: Math. Theor. **47** 175002 (2014)
- 60 M. Kormos, L. Bucciattini, P. Calabrese, EPL **107**, 40002 (2014)
- 61 It is easy to prove that the Wick theorem applies to any eigenstate  $|\psi_0\rangle$  of the local  $\sigma_l^z$ 's operators. Define  $d_l$  annihilation operators as  $c_l$  if  $l$  is in the set of coordinates of an up spin and  $c_l^\dagger$  is vice-versa  $l$  is not in such a set. Analogously define creation operators  $d_l^\dagger$ . It is clear that  $|\psi_0\rangle$  is the vacuum of the fermions  $d_l$ , i.e.  $d_l|\psi_0\rangle = 0, \forall l = 1, \dots, L$  and that the  $d_l$ 's and  $d_l^\dagger$ 's satisfy canonical anticommutation relations. Therefore the Wick theorem applies to correlation functions of the  $d_l$ 's and  $d_l^\dagger$ 's fermions on the state  $|\psi_0\rangle$  and then also to correlation functions of the  $c_l$ 's and  $c_l^\dagger$ 's.
- 62 M. C. Chung and I. Peschel, Phys. Rev. B, **64**, 064412(2001) and I. Peschel, J. Phys. A: Math. Gen. **36**, L205(2003).
- 63 N. Allegra, J. Dubail, J-M. Stéphan and J. Viti, J. Stat. Mech. (2016) 053108.

- <sup>64</sup> J. Viti, J-M. Stéphan, J. Dubail and M. Haque, EPL **115** (2016) 40011.
- <sup>65</sup> The stationary state describing a macroscopic subsystem at infinite time after the quench has been analyzed in great detail in the last decade and we refer the reader to the reviews cited in the Introduction (in particular<sup>32</sup>, sec. III). In brief one can prove for specific models, among which free fermions<sup>21,23</sup>, that the reduced density matrix of a subsystem of length  $l$  at infinite time after the quench coincides in the limit in which the full system is taken infinite ( $L \rightarrow \infty$ ) with the Generalized Gibbs Ensemble constructed from the initial state  $|\psi_0\rangle$ . For  $t \gg l$ ,  $S(t)$  converges to the Von Neumann Entropy of such a mixed state.
- <sup>66</sup> D. Bernard and B. Doyon, J. Stat. Mech. (2016), 064005.
- <sup>67</sup> M. Ljubotina, M. Znidaric and T. Prosen, Nat. Commun. **8**, 16117 (2017).
- <sup>68</sup> J-M. Stéphan, J. Stat. Mech. (2017) 103108.
- <sup>69</sup> M. Collura, A. De Luca and J. Viti, Phys. Rev. B **97**, 081111(R) (2018).
- <sup>70</sup> B. Bertini, L. Piroli and P. Calabrese, [arXiv: 1709.1096].
- <sup>71</sup> B. Bertini, E. Tartaglia and P. Calabrese, [arXiv:1802.10589].
- <sup>72</sup> K. Najafi, M. A. Rajabpour, Phys. Rev. B **96**, 014305 (2017)
- <sup>73</sup> L. Piroli, B. Pozsgay, E. Vernier, [arXiv:1803.04380]